Imaging spectrometry of productive inland waters. Application to the lakes of Mantua

Mariano Bresciani[1], Claudia Giardino[1], Daniele Longhi[2], Monica Pinardi[2], Marco Bartoli[2] and Micòl Vascellari[3]

[1]CNR-IREA, via Bassini 15 - 20133 Milano, Italy. E-mail: bresciani.m@irea.cnr.it
[2]Università di Parma, Dip.to Scienze Ambientali, Parma, Italy
[3]ENAS - Servizio Salvaguardia del Territorio e Tutela delle Acque, Cagliari, Italy

Abstract
In this study remote sensing techniques have been used for small scale analysis of water temperature, chlorophyll *a* (chl-*a*) and total suspended solids (TSS) in three shallow eutrophic lakes (Mantua Lakes, Italy), characterised by variable depths, complex hydrodinamics and elevated primary production of both microalgae and floating leaved macrophytes. Airborne hyperspectral data, acquired in summer 2007, were combined with semi-empirical modelling and provided acceptable estimation of chl-*a* (error 18%) and TSS concentrations (error 24%). The image-derived maps, complemented with the thermal image (error 3%), confirm the hypereutrophic-dystrophic conditions of Mantua Lakes and show the patchy spatial distribution of analysed parameters.
Keywords: productive waters, semi-empirical modelling, imaging spectrometry.

Immagini iperspettrali di acque interne produttive. Applicazione ai laghi di Mantova

Riassunto
In questo studio sono state usate tecniche di telerilevamento per analisi su piccola scala di temperatura, clorofilla a *(chl-*a*) e solidi sospesi totali (TSS) di tre bacini eutrofici poco profondi (Laghi di Mantova, Italia), caratterizzati da profondità variabili, idrodinamismo complesso ed elevata produzione primaria microalgale e macrofitica. Nell'estate 2007 è stata acquisita un'immagine iperspettrale che, mediante modellistica semi-empirica, ha permesso di ottenere mappe di chl-*a *(errore 18%) e TSS (errore 24%) di accettabile accuratezza. Le mappe dei parametri, unitamente all'immagine termica (errore 3%) confermano le condizioni ipertrofiche-distrofiche dei Laghi di Mantova e mostrano la distribuzione a mosaico dei parametri analizzati.*
Parole chiave: *acque produttive, modellistica semi-empirica, immagini iperspettrali.*

Introduction
Wetlands and lakes are precious for wildlife habitat, supporting a rich biodiversity, floodwater management, and water quality improvement as well as having esthetic and educational benefits to humans. Moreover, several local economies depend by water and vegetation

of wetlands and lakes for fisheries, reed harvesting, grazing, and recreation [Barbier et al., 1994]. Unfortunately, in many countries extensive loss of wetlands and the pollution trophic of lake has occurred [Mitsch and Gosselink, 1993]. To prevent further loss and ensure the safeguard existing wetland ecosystems for biodiversity and ecosystem services and goods, it is essential to catalogue and monitor wetlands, their contiguous uplands, and its water component, as the state of conservation of wetlands is strictly connected to the status of their waters [Schröder, 1979; Van der Putten et al., 1997].

To this aim, remote sensing has some advantages as it can be used for those inaccessible wetlands as well as to assess their directional changes [Lyon and Greene, 1992; Jensen et al., 1993], by seasonally- or yearly-based observations [Ozesmi and Bauer, 2002]. Since the '80, remote sensing techniques are extensively adopted for the characterisation of optically-active water parameters in aquatic bodies as seas and oceans. Ocean colour remote sensing permits to monitor the water component of wetlands, as it has been proved its capabilities in retrieving water quality parameters not only in oceans but also in coastal zones, lakes, lagoons and in general in inland waters [e.g., Lindell et al., 1999]. In recent years, new developments in water quality algorithms have mainly been driven by the advent of MODIS and MERIS satellite sensors and their specific capacities to asses the low radiances emerging from water bodies. Nevertheless, a spatial resolution of 1000 m (MODIS) or even 300 m (MERIS) can be still inadequate for small size water bodies which can be instead imaged from airborne sensors.

Imaging spectrometry offers a versatile tool for assessing water quality in small lakes [e.g., George, 1997], to monitor the variation of submerged vegetation in coastal zones [e.g., Giardino et al., 2007] and to perform ad hoc studies in transitional ecosystems as lagoons [e.g., Alberotanza et al., 1999]. In shallow lakes and wetlands the successful application of remote sensing techniques can clarify complex dynamics between primary producers, track their evolution, evidence complex patterns in the distribution of microalgae and suspended material, map macrophytic vegetation and its dynamics, providing useful information to ecologist and environmental managers. However, remote sensing of small lakes and wetlands require detailed calibration activities performed on wide range of concentrations, and robust modelling, accounting for dramatic changes of water features in time and space. Such changes are due to fast growing emergent vegetation in the littoral zones or forming islands within the water body, altering water circulation patterns, the sedimentation-resuspension of particulate matter and, via a number of competitive mechanisms, phytoplankton blooms.

In this work we present data from the eutrophic shallow lakes of Mantua (northern Italy); imaging spectrometry and semi-analytical modelling were used to map chlorophyll *a* and total suspended solids concentrations and water surface temperature.

Material and methods

Study area

The lakes of Mantua (Upper, Middle and Lower) are three small and shallow basins surrounding the city of Mantua (Fig. 1, Tab. 1). The lakes are fed by the Mincio River, which is the emissary of Lake Garda. The current hydraulic system regulating the course of the river around the town dates back to the year 1190. The level of the three lakes is controlled by the Vasarone dam (Fig. 1) to guarantee a water level of 17.5 m a.s.l. in the Lake Upper and of 14.4 m a.s.l. in the Middle and Lower lakes. The Mincio River has an

average annual (2000-2006) flow of 20±6 m^3s^{-1}, corresponding to a residence time of water in the three lakes of about 8.4, 1.9 and 2.5 days, respectively.

Table 1 - Main features of the three lakes of Mantua [Osservatorio dei laghi Lombardi, 2005].

Lake	Lake area [km^2]	Perimeter [km]	Storage volume [$\times 10^6$ m^3]	Mean depth [m]
Upper	3.67	10	14.5	3.6
Middle	1.09	6	3.27	3.0
Lower	1.45	6	4.36	3.3

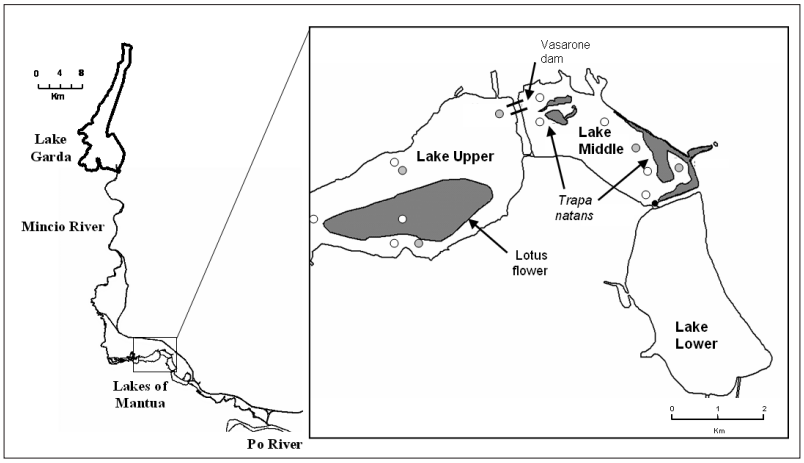

Figure 1 - Map of the study area. Grey dots indicate the field stations measured on June 26, 2007, in white the stations (one in the Lotus flower island) measured on July 26, 2007, synchronously to the image acquisition.

The three lakes are characterised by eutrophic levels, problematic organic matter sedimentation and excess growth of macrophitic vegetation. From spring to autumn, a large part of the surface of the lakes is covered by dense stands of emergent macrophytes such as the common water chestnut (*Trapa natans*) and the lotus flower (*Nelumbo nucifera*), an exotic invasive species introduced at the beginning of the 20th century.

Field data and modelling

Two field campaigns were conducted on June 26 and on July 26, 2007 for a total of 14 investigated stations, distributed in the Upper and Middle lakes. At each station, water samples were collected near surface and filtered *in situ* for subsequent laboratory analysis. Chlorophyll *a* (chl-*a*) concentrations were determined according to trichromatic method [APHA, 1981]. Total suspended solids (TSS) concentrations were determined gravimetrically [Strömbeck and Pierson, 2001]. The *in situ* measured surface temperature ranged from 24.7 °C to 26.7 °C.

Widely variable water components conditions were encountered in the study area: chl-*a* concentrations varied between 58 and 214 mgm^{-3} and TSS concentrations between 13 and 32 gm^{-3}. As shown in Figure 2, chl-*a* and TSS were not related, confirming that the lakes of Mantua are typical case-2 waters [Morel and Prieur, 1977].

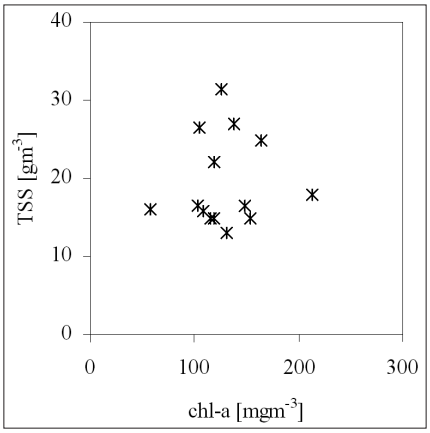

Figure 2 - TSS concentrations plotted versus and chl-*a* concentrations; the poor correlation (r=0.0007) is typical of case-2 waters.

At the same stations of water sampling, remote sensing reflectance (Rrs) (the wavelength dependence is omitted for clarity if not for a few exceptions) values were derived by underwater down-welling irradiance and up-welling radiance measurements, subsequently corrected for the emersion factor. The Rrs spectra in the 450-750 nm wavelength range are plotted in Figure 3. The spectra were quite similar in magnitude to typical reflectance spectra collected in other turbid productive waters [Dall'Olmo and Gitelson, 2006]. The reflectance in the red-near infrared regions was the same in magnitude, or even higher, as the green reflectance peak.

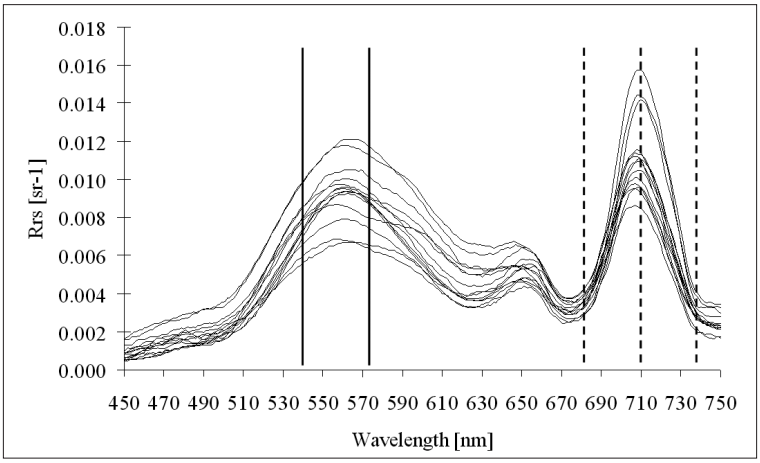

Figure 3 - In situ measured Rrs spectra; the two continuous lines indicate the position of MIVIS bands used to apply the band-ratio model for TSS; the three dotted lines indicate the position of MIVIS channels used to apply the three-bands model for chl-*a*.

The magnitude and shapes of *in situ* spectra were then used to parameterise semi-analytical models to retrieve chl-*a* and TSS concentrations from Rrs band combinations.
The three-band model [Gitelson et al., 2007 and references herein] of the form [$Rrs^{-1}(\lambda 1)$-$Rrs^{-1}(\lambda 2)$]×Rrs(λ3) , where Rrs(λi) is the Rrs at the wavelength λi was adopted to retrieve chl-*a* concentrations. The best combination of spectral bands selected by model tuning (Fig. 4) was the following:

$$\text{chl-}a = 170.81 \times [Rrs^{-1}(677) - Rrs^{-1}(710)] \times Rrs(747) + 36.105 \quad [mgm^{-3}] \quad [1]$$

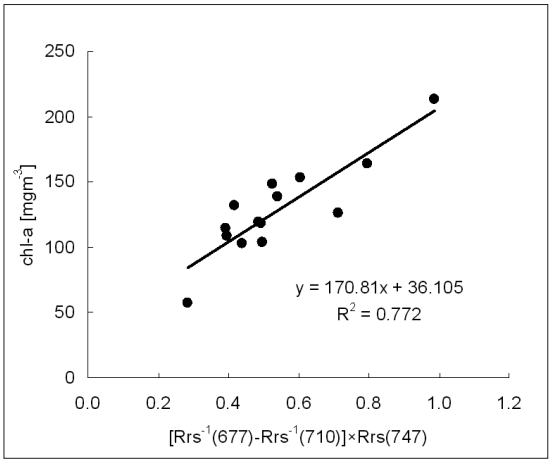

Figure 4 - Three-band model (equation 1) plotted versus laboratory measurements of chl-*a* concentrations. The lowest chl-*a* concentration was measured in the station within the lotus flower island (cf. Fig. 1).

The model for TSS concentrations was derived by using band ratios. The ratios of each of the Rrs wavelengths against each other was calculated and linearly correlated with TSS concentrations, allowing the identification of any channel ratios that showed a high correlation with TSS. The value of the regression coefficient R^2, between the ratio of each pair of channels and the concentrations of TSS is displayed as a matrix (Fig. 5, left). Three regions were identified as most significantly correlated (R^2>0.6) with TSS: around 720/710, 720/600 and 540/570, respectively. The two ratios around 700 were excluded because in that region the behaviour Rrs is influenced by phytoplankton absorption, whereas in the 540/570 region the absorption due to phytoplankton is minimum. The best combination of spectral bands in the band-ratio model (Fig. 5, right) was the following:

$$TSS = 141.78 \times [Rrs^{-1}(542) \times Rrs(575)] - 121.53 \quad [gm^{-3}] \quad [2]$$

MIVIS data

On July 26, 2007, Multispectral Infrared and Visible Imaging Spectrometer (MIVIS) data were acquired with a spatial resolution of 4 m × 4 m, with Sun elevation of 63°.

Unfortunately the optimal view conditions for water targets (e.g., sun elevations between 35° and 50° and orientation of the sensor toward or away from the sun) [Mustard et al., 2001] were not achieved in this flight and glint patterns were visible in some portion of the image. The method proposed by Hochberg et al. [2003] to correct for glint effects was tested (not shown here) but any significant improvement was obtained, probably because the difficult to find a sufficient large area of homogenous water. Glint patterns were hence masked with clouds. Then, at-the-sensor radiances were converted into water Rrs values by using the empirical-line method calibrated with *in situ* reflectance spectra, while thermal channels were not corrected for the atmospheric effects.

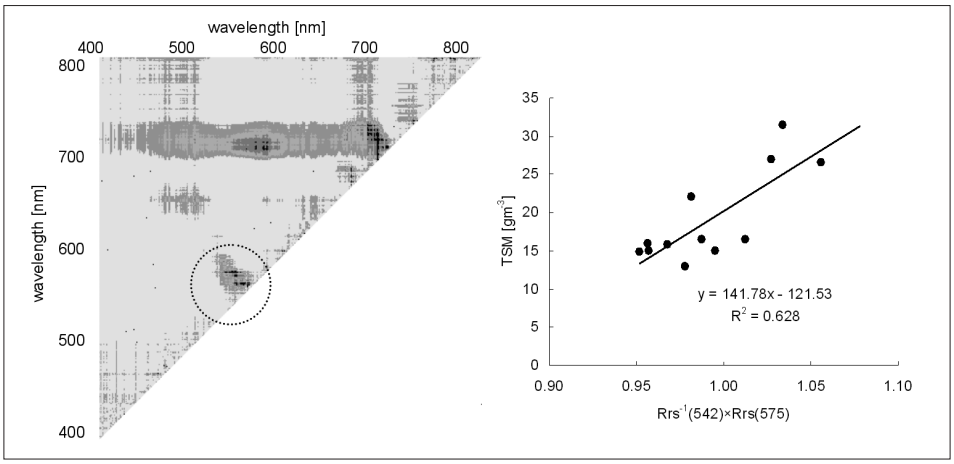

Figure 5 - Left: the correlation matrix shows (R^2 increases from grey to black) the best combination of Rrs measurements to include in a band-ratio algorithm to estimate TSS concentrations in the study area. Right: the band-ratio model [2] plotted versus laboratory measurements of TSS concentrations.

MIVIS images of Rrs values were then converted into water quality products. The three-band model for chl-*a* was applied to MIVIS-derived Rrs data in bands 13, 14 and 16, overlapping the three wavelengths 677, 710 and 747 nm of equation 1, respectively. Similarly, the band-ratio model for TSS was applied to MIVIS-derived Rrs data in bands 6 and 8, overlapping the two wavelengths 542, and 575 nm of equation 2, respectively.
Raw MIVIS channel 96 was used to map the surface temperatures patterns.

Results and discussion

Figure 6 shows the MIVIS-derived water quality products on July 26, 2007. The products were validated using *in situ* data of Lake Middle stations (cf. Fig. 1), which were collected within 3 hours of the sensor overpass. Table 2 shows the comparison of MIVIS-derived values and *in situ* measurements, with root means square errors, both absolute (RMSE) and relative (RMSE%). The highest RMSE (24%) was observed for TSS, while the lowest for temperature (3%).

Table 2 - Comparison of *in situ* measured and MIVIS derived water quality parameters. The last rows indicate the root means square errors, absolute (RMSE) and relative to average *in situ* data (RMSE%).

	chl-*a* [mgm^{-3}]		TSS [gm^{-3}]		Temperature [°C]	
	In situ	**MIVIS**	**In situ**	**MIVIS**	**In situ**	**MIVIS**
	148.1	138.0	16.5	17.0	26.4	26.2
	102.9	103.8	16.5	19.0	26.7	26.3
	117.9	108.4	22.0	18.0	27.0	26.2
	152.9	111.9	15.0	15.0	26.9	26.0
	131.7	110.8	13.0	19.6	25.9	25.4
	148.1	138.0	16.5	17.0	26.4	26.2
	148.1	138.0	16.5	17.0	26.4	26.2
RMSE	24.0		4.1		0.7	
RMSE %	18%		24%		3%	

The chl-*a* map (Fig. 6, top), which was obtained by applying the three-band model independently developed by using field data, shows a range between 80 and 140 mgm^{-3}. Lake Upper areas closer to the Mincio River inlet exhibit highest chl-*a* concentrations, with chl-*a* patterns decreasing in the central portion of this lake, nearby the lotus flower island. Phytoplankton growth is likely limited by light availability within the lotus island; alternatively, the dense stems of the macrophyte reduce locally the water flow and enhance the sedimentation rates of suspended matter. In Lake Middle, chl-*a* concentrations are slightly lower, with an average of 110 mgm^{-3}, and exhibit a more homogenous pattern. Lake Lower is characterized by lowest values of chl-*a* (around 80 mgm^{-3}). However, glint, clouds and the absence of *in situ* data limit the analysis in this lake. The TSS map (Fig. 6, middle) shows concentrations varying between 10 and 30 gm^{-3} and reveal higher concentrations in Lake Upper than in Lake Middle. As for chl-*a*, the TSS map of Lake Lower is strongly disturbed by different source of noise (clouds and glint). The map of surface temperature (Fig. 6, bottom) is quite homogenous with the exception of a northern area in Lake Middle, which is interested by the discharge of warmer waters from a paper mill.

The Mincio River transports to the lakes of Mantua high loads of suspended particles and nutrients that fuel phytoplankton growth, but microalgal blooms are controlled by a number of factors [Telò et al., 2007]. In the period of this investigation the water flow from the Mincio River was at its minimum (<5 m^{3}s^{-1}) due to withdrawal for irrigation purposes and water shortage in the Lake Garda, resulting in longer water renewal in the Mantua Lakes and irrelevant water speed, favouring sedimentation. Very high chl-*a* values as those reported in the present study result in self limitation of phytoplankton due to extremely limited light penetration in the water column, in particular under stagnation conditions. Pinardi et al., in preparation, have demonstrated that phytoplanktonic primary production is enhanced by water flow, exporting particles downstream and keeping high the potential for algal growth. Under more dynamic conditions, chl-*a* values tend to increase downstream, whilst the opposite was evidenced in this study. Furthermore, macrophytic vegetation attains in July the peak of biomass, and has the potential to inhibit at least partially phytoplankton growth due to water column shading, nutrient uptake or production of allelochemicals. A

combination of reduced flow and macrophitic vegetation peak can explain the chl-*a* and TSS decreasing trend from the Upper to the Lower Lakes.

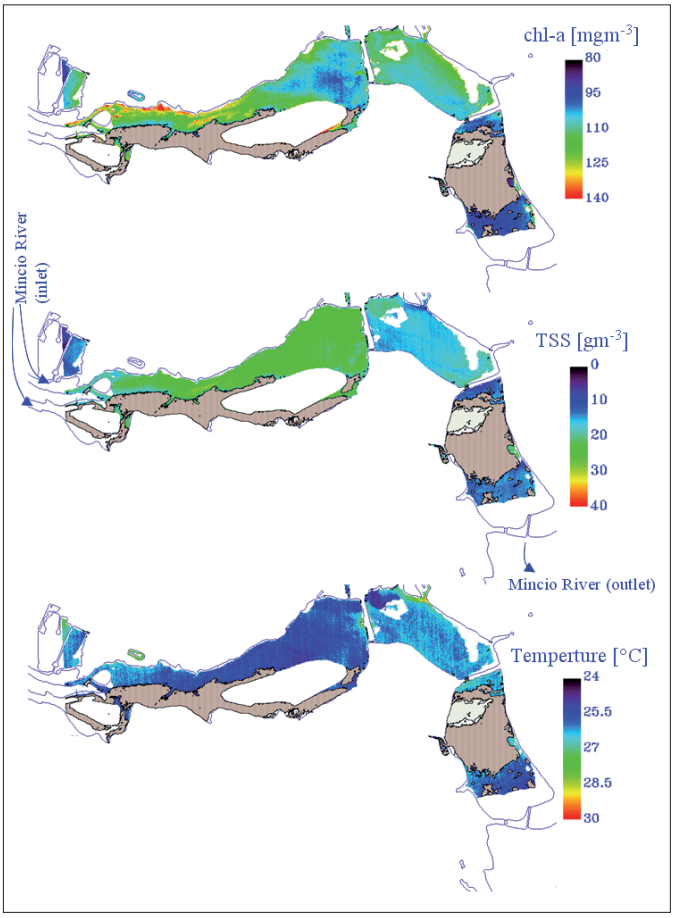

Figure 6 - MIVIS-derived water quality maps of three lakes of Mantua (from left to right: Upper, Middle and Lower). From top to bottom: chl-*a*, TSS and surface temperature. Glint (dark grey), clouds (light grey) and macrophytes (white) are masked. The Mincio River inlet/outlet are indicated in the TSS map.

Conclusions

In this study semi-empirical modelling independently developed by using *in situ* data was applied to MIVIS data of lakes of Mantua. The proposed method was accurate in describing the spatial patterns of chl-*a* (RMSE 18%), TSS (RMSE 24%) and surface temperature (RMSE 3%). The chl-*a* and the TSS maps confirmed the hypereutrophic-dystrophic conditions of the lakes of Mantua and the elevated load of nutrient and suspended matter transported by the Mincio River to the lakes. The surface temperature map revealed the discharge of warmer waters by a paper mill. These results may be combined with studies on aquatic vegetation,

water flow and bathymetry of the study area for a more complete assessment of ecological features of the entire wetland. Vascellari et al. [2008] used MIVIS data to determine the extension of macrophytes growing in the study area. Future acquisitions of MIVIS data are recommended to verify the hypothesis about the role of Mincio River flow and vegetation island development in regulating the patterns of suspended matter and phytoplankton distribution. By also considering that one or two scenes can be used for synoptic studies of the whole ecosystem, early spring and summer applications of the proposed method will also contribute in implementing the Water Framework Directive [2000/60/EC] relatively both to inventory of macrophytes and to water quality assessment.

Acknowledgements

We are very grateful to A. Gitelson for his proficient feedback on field data collected in the study area. MIVIS data were acquired by CGR-CISIG Parma (Italy).

References

Alberotanza L., Brando V.E., Ravagnan G., Zandonella A. (1999) - *Hyperspectral aerial images. A valuable tool for submerged vegetation recognition in the Orbetello Lagoons, Italy*. Int. J. of Remote Sens., 20: 523-533.

APHA (1981) - *APHA, AWWA, WPCF Standard Methods for the Examination of Water and Wastewater*. 15th edition. American Public Health Association. Washington, D.C., 1134 pp.

Barbier E.B., Burgess J.C., Folke C. (1994) - *Paradise Lost? The Ecological Economics of Biodiversity*. Earthscan, London, 267 pp.

Dall'Olmo G., Gitelson A.A. (2006) - *Effect of bio-optical parameter variability on the remote estimation of chlorophyll-a concentration in turbid productive waters: experimental results*. App. Opt., 44: 412-422.

Directive 2000/60/EC (2000) - *Water Framework Directive of the European Parliament and of the Council of 23 October 2000 establishing a framework for Community action in the field of water policy*. Official Journal L 327, 22 December 2000.

George D.G. (1997) - *The airborne remote sensing of phytoplankton chlorophyll in the lakes and tans of the English Lake District*. Int. J. of Remote Sens, 18: 1961-1975.

Giardino C., Bartoli M., Candiani G., Bresciani M., Pellegrini L. (2007) - *Recent changes in macrophyte colonisation patterns: an imaging spectrometry-based evaluation of southern Lake Garda (northern Italy)*. J. of App. Rem. Sens. (SPIE), Vol. 1, 011509.

Gitelson A.A., Schalles J.F., Hladik C.M. (2007) - *Remote chlorophyll-a retrieval in turbid, productive estuaries: Chesapeake Bay case study*. Remote Sens. of Environ., 109: 464-472.

Hochberg E.J., Andréfouët S., Tyler M.R. (2003) - *Sea surface correction of high spatial resolution Ikonos images to improve bottom mapping in near-shore environments*. IEEE Trans. on Geosc. and Remote Sens., 41: 1724-1729.

Jensen J., Narumalani S., Weatherbee O., Mackay H.E. (1993) - *Measurement of seasonal and yearly cattail and waterlily changes using multidate SPOT panchromatic data*. Photogram. Eng. & Remote Sens., 59: 519-525.

Lindell T., Pierson D., Premazzi G., Zilioli E. (1999) - *Manual for monitoring European lakes using remote sensing techniques*. Luxembourg: Office for Official Publications of

the European Communities, EUR Report n. 18665 EN, 164 pp.
Lyon J.G., Greene R.G. (1992) - *Use of aerial photographs to measure the historical areal extent of Lake Erie coastal wetlands*. Photogram. Eng. & Remote Sens., 58: 1355-1360.
Mitsch W.J., Gosselink J.G. (1993) - *Wetlands*. 2nd edn. Van Nostrand Reinhold, New York, 722 pp.
Morel A., Prieur L. (1977) - *Analysis of variations in ocean color*. Limn. and Oceano., 22: 709-722.
Mustard J.F., Staid M.I., Fripp W.J. (2001) - *A semianalytical approach to the calibration of AVIRIS data to reflectance over water application in a temperate estuari*. Remote Sens. of Environ., 75: 335-349.
Osservatorio dei Laghi Lombardi (2005) - *Qualità delle acque lacustri in Lombardia, 1° Rapport OLL 2004*. Regione Lombardia, ARPA Lombardia, Fondazione Lombardia per l'Ambiente e IRSA/CNR, 2005 (ISBN 88-8134-085-2).
Ozesmi S.L., Bauer M.E. (2002) - *Satellite remote sensing of wetlands*. Wetlands Ecology and Management, 10: 381-402.
Schröder R. (1979) - The decline of reed swamps in Lake Constance. *Symp Biol Hung*, 19: 43-48.
Strömbeck N., Pierson E. (2001) - *The effects of variability in the inherent optical properties on estimations of chlorophyll a by remote sensing in Swedish freshwater*. Sci. of the Tot. Environ., 268: 123-137.
Telò R., Pinardi M., Bartoli M., Bodini A., Viaroli P., Racchetti E., Cuizzi D., Vannuccini M., Previdi L. (2007) - *Caratterizzazione dello stato ambientale del fiume Mincio e analisi della strategia di riqualificazione integrata e partecipata*. Relazione Forum del Mincio.
Van der Putten W.H., Peters B.A.M., Van den Berg M. S. (1997) - *Effect of litter on substrate conditions and growth of emergent macrophytes*. New Phytologist, 135: 527-537.
Vascellari M., Giardino C., Bresciani M., Longhi D., Bartoli M., Dessena M.A. (2008) - *Il contributo del MIVIS nello studio ecologico delle acque e della vegetazione dei laghi di Mantova*, 12a Conferenza Nazionale ASITA, L'Aquila, Italy, 21-24 October 2008: 1893-1898.

Received 13/03/2009, accepted 7/04/2009.